Discussion Paper No.240

Nonlinear Cournot Duopoly with Implementation Delays

Akio Matsumoto
Chuo University

Ferenc Szidarovszky
University of Pécs

January 2015

INSTITUTE OF ECONOMIC RESEARCH
Chuo University
Tokyo, Japan

Nonlinear Cournot Duopoly with Implementation Delays*

Akio Matsumoto† Ferenc Szidarovszky‡

Abstract

We study the effects of two delays on the local as well as on global stability of nonlinear Cournot duopoly dynamics. The two major findings are an analytical construction of the stability switching curve on which stability is lost and the numerical confirmation of the birth of aperiodic global dynamics when the stationary state is locally unstable. The delays matters and can generate various dynamics ranging from simple to complicated dynamics.

Keywords: Implementation delays, Gradient dynamics, Stability switches, Cournot duopoly, Hopf bifurcation

*The authors highly appreciate the financial supports from the MEXT-Supported Program for the Strategic Research Foundation at Private Universities 2013-207, the Japan Society for the Promotion of Science (Grant-in-Aid for Scientific Research (C) 24530202, 25380238 and 26380316). The usual disclaimers apply.

†Professor, Department of Economics, Senior Researcher, International Center for further Development of Dynamic Economic Research, Chuo University, 742-1, Higashi-Nakano, Hachioji, Tokyo, 192-0393, Japan; akiom@tamacc.chuo-u.ac.jp

‡Professor, Department of Applied Mathematics, University of Pécs, Ifjúság, u. 6, H-7624, Pécs, Hungary; szidarka@gmail.com

1 Introduction

Oligopoly theory has a long history since the pioneering work of Cournot (1838). It has played a central role in mathematical economics and developed in various directions. The existence and uniqueness of the equilibrium were the research issues in early stage and then dynamic extensions become the main topic of researchers. Linear models were first examined, where local asymptotical stability implies global stability. Each model is based on a particular output adjustment scheme. In applying best response dynamics, global information is needed about the profit function while in the case of gradient adjustments only local information is needed to assess the marginal profit. Okuguchi (1976) summarizes the early results on static and dynamic oligopolies and Okuguchi and Szidarovszky (1999) discuss their multiproduct generalizations. During the last two decades an increasing attention has been given to nonlinear dynamics. Bischi et al. (2010) give a comprehensive summary of the newer developments. Concerning oligopoly dynamics, it is now well-known that oligopoly models formulated in discrete-time framework can generate various dynamics ranging from simple dynamics to complex dynamics including chaos if endogenous nonlinearities become stronger. It is also well-known that continuous-time oligopoly models behave better than discrete-time models in a sense that the former models have larger stability regions of the parameters. In the existing literature, however, not much has been revealed with the delay oligopoly model that is a hybrid of the discrete-time and the continuous-time models.[1] In particular, it has not yet been known what dynamic behavior arises when more than one delays are involved in economic variables.

The main purpose of this paper is to provide rigorous theoretical analysis on multiple-delay dynamic behavior and to confirm the analytical results by performing numerical simulations. For this end, we construct an *á la* Cournot duopoly model in which each firm has a delay in implementing information about its own output. This is a continuity of Matsumoto *et al.* (2011) in which a linear duopoly model with two fixed delay is considered. It is a special case of Howroyd and Russell (1984) in a sense that the number of the firms is reduced to two from a general N and, at the same time, considered to be an extended case in a sense that the number of delays is increased to two from one. It is also an application of the results obtained in delay dynamic monopolies of Matsumoto and Szidarovszky (2014a, b). We apply an analytical method developed by Lin and Wang (2012) and construct a *stability switching curve* with respect to two delays. We provide some examples in which periodic as well as aperiodic delay dynamics may appear in a 2D system of differential equations.

The paper is organized as follows. In Section 2, the traditional continuous-time duopoly model is presented and then delays are implemented. The stability switching curves are analytically derived. In Section 3, we give numerical ex-

[1] The delay equations describing the population of the species are frequently discussed in theoretical biology. Even in early 80s, Shibata and Saito (1980) investigate the time delayed saturation effect in a logistic model of two competing species and numerically confirm the birth of chaotic solutions.

amples to illustrate the theoretical findings and to find how the delays affect dynamic behavior. In the final section, concluding remarks are given.

2 Delay Model

We consider an industry of two firms producing a homogeneous good. Let x and y be the output quantities produced by firms x and y, respectively. The price function is assumed to be linear,

$$p = a - b(x + y) \text{ with } a > 0 \text{ and } b > 0.$$

Production costs are also assumed to be linear and the marginal costs are denoted by c_x and c_y. The profit function of firm z ($z = x, y$) is given by

$$\pi_z = (a - b(x + y))z - c_z z.$$

Firm z determines its output to maximize profit, taking quantity supplied by the competition as given. Assuming an interior optimal solution and solving the first-order condition for the profit maximizing problem yield the best replies (or reaction functions),

$$R_x(y) = \frac{1}{2}(a - c_x - by) \text{ and } R_y(x) = \frac{1}{2}(a - c_y - bx).$$

A Cournot equilibrium is a pair of outputs (x^e, y^e) satisfying $x^e = R_x(y^e)$ and $y^e = R_y(x^e)$, that is,

$$x^e = \frac{a - 2c_x + c_y}{3b} \text{ and } y^e = \frac{a - 2c_y + c_x}{3b}$$

where the following is assumed to guarantee positive equilibrium,

$$a > \max[2c_x - c_y,\ 2c_y - c_x].$$

Concerning the adjustment process of output, we make two assumptions. One is that the firms are boundedly rational in a sense that they modify their production according to the sign of the marginal profits. That is, the firm increases its production if the marginal profit is positive, decreases it if negative and does not change it if zero. Such an adjustment process is called gradient dynamics and satisfies the following condition,

$$sign\left[\dot{z}(t)\right] = sign\left[\frac{d\pi_z}{dz}\right].$$

Specifically, two formulations are often used,

$$\frac{\dot{z}(t)}{z(t)} = k_z \frac{d\pi_z}{dz} \text{ or } \dot{z}(t) = f_z(z)\frac{d\pi_z}{dz} \text{ with } f_z'(z) > 0,$$

where the growth rate of the variable is portional to the marginal profit in the first formulation and the adjustment rate is determined in the second formulation by a product of the marginal profit and the degree of the adjustment that depends on the level of the variable. Notice that the two are mathematically equivalent if $f_z(z) = k_z z$ although their economic interpretations are different. The other assumtption is that the firms obtain only delayed information on production activities. There are two ways to introduce a delay in our framework. The first is a delay in implementing information about firm's own output and the second is a delay in obtaining information about the competitor's output. However, it has been shown by Howroyd and Russell (1984) that the second delay is harmless in a Cournot oligopoly model.[2] Thus we focus on only the first delay in this study to simplify the analysis. The two assumptions can be given in the following way.

Assumption 1. The firms continuously adjust their output growth rates proportional to changes in their profits.

Assumption 2. The firms experience delays in implementing information about their own outputs.

With positive adjustment coefficients α_x and β_y of firms x and y, this gradient dynamic system is described by a 2D system of delay differential equations,

$$\begin{aligned} \dot{x}(t) &= \alpha_x x(t) \left[a - c_x - 2bx(t-\tau_x) - by(t)\right], \\ \dot{y}(t) &= \beta_y y(t) \left[a - c_y - bx(t) - 2by(t-\tau_y)\right], \end{aligned} \tag{1}$$

where $\tau_x \geq 0$ and $\tau_y \geq 0$ are time delays. The positive steady state of system (1) is identical with Cournot equilibrium (x^e, y^e).[3] The linear approximation in a neighborhood of the equilibrium is

$$\begin{aligned} \dot{x}_\delta(t) &= \alpha \left[-2bx_\delta(t-\tau_x) - by_\delta(t)\right], \\ \dot{y}_\delta(t) &= \beta \left[-bx_\delta(t) - 2by_\delta(t-\tau_y)\right], \end{aligned} \tag{2}$$

where

$$x_\delta(t) = x(t) - x^e,\ y_\delta(t) = y(t) - y^e,\ \alpha = \alpha_x x^e \text{ and } \beta = \beta_y y^e.$$

Substituting exponential solutions

$$x(t) = e^{\lambda t} u \text{ and } y(t) = e^{\lambda t} v,$$

[2] A more general result obtained in Hofbauer and So (2000).

[3] This model has multiple equilibria. Other than the positive equilibrium, there are one zero solution and two corner solutions that correspond to monopoly equilibrium. Our concern is on the positive equilibrium in this study.

into the linearized equations in (2) and arranging terms yield a 2D simultaneous equation system with respect to u and v,

$$\begin{pmatrix} \lambda + 2\alpha b e^{-\lambda\tau_x} & \alpha b \\ \beta b & \lambda + 2\beta b e^{-\lambda\tau_y} \end{pmatrix} \begin{pmatrix} u \\ v \end{pmatrix} = \begin{pmatrix} 0 \\ 0 \end{pmatrix}.$$

Thus the corresponding characteristic equation is

$$P(\lambda, \tau_x, \tau_y) = P_0(\lambda) + P_1(\lambda)e^{-\lambda\tau_x} + P_2(\lambda)e^{-\lambda\tau_y} + P_3(\lambda)e^{-\lambda(\tau_x+\tau_y)} = 0 \quad (3)$$

where

$$P_0(\lambda) = \lambda^2 - \alpha\beta b^2,$$

$$P_1(\lambda) = 2\alpha b\lambda,$$

$$P_2(\lambda) = 2\beta b\lambda,$$

$$P_3(\lambda) = 4\alpha\beta b^2.$$

Before proceeding, we examine the non-delay case with $\tau_x = \tau_y = 0$ in which case the characteristic equation is simplified as

$$\lambda^2 + 2b(\alpha + \beta)\lambda + 3b^2\alpha\beta = 0.$$

Since all coefficients of this equation and the discriminant are positive, the characteristic roots are real and negative, implying that the steady state with no delays is locally stable. We can mention that it is still stable as long as positive delays are sufficiently small by continuous dependency of λ on the values of delays. To see what extent the stationary point can preserve stability, we determine the threshold values of the delays for which stability is just lost.

The characteristic equation (3) is now investigated with a constructive method developed by Lin and Wang (2012) to solve a class of two delay differential equations. We look for a pair of the delays for which the characteristic equation has purely imaginary roots. The set of such pairs is called *stability switching curve*. Since $\lambda = 0$ is not a solution and roots of a real function come in conjugate pairs, we assume, without loss of generality, that $\lambda = i\omega$ with $\omega > 0$ on this curve. Substituting this solution into (3), we have two different forms,

$$\left[P_0(i\omega) + P_1(i\omega)e^{-i\omega\tau_x}\right] + \left[P_2(i\omega) + P_3(i\omega)e^{-i\omega\tau_x}\right] e^{-i\omega\tau_y} = 0 \quad (4)$$

and

$$\left[P_0(i\omega) + P_2(i\omega)e^{-i\omega\tau_y}\right] + \left[P_1(i\omega) + P_3(i\omega)e^{-i\omega\tau_y}\right] e^{-i\omega\tau_x} = 0 \quad (5)$$

Using equations (4) and (5), we can derive the following theorem that yields explicit expressions for the stability switching curves.

Theorem 1 *Suppose that* $P_2\bar{P}_3 - P_0\bar{P}_1 \neq 0$ *and* $P_1\bar{P}_3 - P_0\bar{P}_2 \neq 0$. *Then the stability switching curves are the loci of* $L_R(m,n)$ *and* $L_B(m,n)$ *defined by*

$$L_R(m,n) = \left\{ (\tau_x^+(\omega,m), \tau_y^-(\omega,n)) \;\middle|\; \omega \in \Omega^1,\ m,n \in \mathbb{Z} \right\}$$

and

$$L_B(m,n) = \left\{ (\tau_x^-(\omega,m), \tau_y^+(\omega,n)) \;\middle|\; \omega \in \Omega^2,\ m,n \in \mathbb{Z} \right\}$$

where Ω^1 *and* Ω^2 *are the sets of* $\omega > 0$ *for which relations (A-5) and (A-6)/of the Appendix are satisfied, furthermore*

$$\tau_x^{\pm}(\omega,m) = \frac{\pm\psi_x(\omega) - \varphi_x(\omega) + 2m\pi}{\omega},$$

and

$$\tau_y^{\pm}(\omega,n) = \frac{\pm\psi_y(\omega) - \varphi_y(\omega) + 2n\pi}{\omega},$$

with $\varphi_x(\omega) = \arg(P_2\bar{P}_3 - P_0\bar{P}_1)$, $\varphi_y(\omega) = \arg(P_1\bar{P}_3 - P_0\bar{P}_2)$,

$$\psi_x(\omega) = \cos^{-1}\left[\frac{|P_0|^2 + |P_1|^2 - |P_2|^2 - |P_3|^2}{2\,|B_1(\omega)|}\right],\ \psi_x \in [0,\pi],$$

and

$$\psi_y(\omega) = \cos^{-1}\left[\frac{|P_0|^2 - |P_1|^2 + |P_2|^2 - |P_3|^2}{2\,|B_2(\omega)|}\right],\ \psi_y \in [0,\pi].$$

Proof. Proof is given in the Appendix. ■

To check the existence and domain of ω for which inequalities (A-5) and (A-6) (given in the Appendix) hold, we introduce two functions,

$$F(\omega) = \left(|P_0|^2 + |P_1|^2 - |P_2|^2 - |P_3|^2\right)^2 - 4B_1^2 \leq 0$$

and

$$G(\omega) = \left(|P_0|^2 - |P_1|^2 + |P_2|^2 - |P_3|^2\right)^2 - 4B_2^2 \leq 0.$$

It can be shown that the right hand side expressions of $F(\omega)$ and $G(\omega)$ are equivalent and, with the notation of $z = \omega/b$, are reduced to

$$z^8 + 4a_3z^6 + 2a_2z^4 + 4a_1z^2 + a_0$$

where

$$a_3 = -2\alpha^2 + \alpha\beta - 2\beta^2,$$

$$a_2 = 8\alpha^4 + 8\alpha^3\beta - 19\alpha^2\beta^2 - 8\beta^4 + 16\alpha^2\beta(4\beta - \alpha),$$

$$a_1 = -30\alpha^4\beta^2 - 15\alpha^3\beta^3 + 30\alpha^2\beta^4 - 4\alpha^2\beta^2(4\beta - \alpha)^2,$$

$$a_0 = 225\alpha^4\beta^4.$$

Let $Z = z^2$ and

$$f(Z) = Z^4 + 4a_3Z^3 + 2a_2Z^2 + 4a_1Z + a_0.$$

Solving $f(Z) = 0$ for Z yields four solutions,

$$Z_1 = 2\alpha^2 - \alpha\beta + 2\beta^2 + 2\,|\alpha - \beta|\,\sqrt{\alpha^2 + \alpha\beta + \beta^2},$$

$$Z_2 = 2\alpha^2 - \alpha\beta + 2\beta^2 - 2\,|\alpha - \beta|\,\sqrt{\alpha^2 + \alpha\beta + \beta^2},$$

$$Z_3 = 2\alpha^2 - \alpha\beta + 2\beta^2 + 2\,|\alpha - \beta|\,\sqrt{\alpha^2 - 3\alpha\beta + \beta^2},$$

$$Z_4 = 2\alpha^2 - \alpha\beta + 2\beta^2 - 2\,|\alpha - \beta|\,\sqrt{\alpha^2 - 3\alpha\beta + \beta^2}.$$

Let us denote the discriminant of the last two equations by $D = \alpha^2 - 3\alpha\beta + \beta^2$. Notice that Z_3 and Z_4 are real if $D \geq 0$ and complex if $D < 0$, and the following result is the simple consequence of the above expressions:

Lemma 1 *Given $\alpha > 0$ and $\beta > 0$,*

$$\begin{aligned}
&\textit{If } \alpha = \beta, && \textit{then } 0 < Z_1 = Z_2 = Z_3 = Z_4;\\
&\textit{If } \alpha \neq \beta \textit{ and } D \geq 0, && \textit{then } 0 < Z_2 < Z_4 \leq Z_3 < Z_1;\\
&\textit{If } \alpha \neq \beta \textit{ and } D < 0, && \textit{then } 0 < Z_2 < Z_1.
\end{aligned}$$

This lemma immediately implies the following result:

Theorem 2 *Given $\alpha > 0, \beta > 0$ and $b > 0$,*

$$\begin{aligned}
&\textit{If } \alpha = \beta, && \textit{then } F(\omega) \geq 0 \textit{ for all } \omega \geq 0;\\
&\textit{If } \alpha \neq \beta \textit{ and } D \geq 0, && \textit{then } F(\omega) \leq 0 \textit{ for } \omega \in [\omega_2, \omega_4] \textit{ and } \omega \in [\omega_3, \omega_1];\\
&\textit{If } \alpha \neq \beta \textit{ and } D < 0, && \textit{then } F(\omega) \leq 0 \textit{ for } \omega \in [\omega_2, \omega_1]
\end{aligned}$$

where for $i = 1, 2, 3, 4$,

$$\omega_i = z_i b \textit{ with } z_i = \sqrt{Z_i}.$$

In examining the sign of the discriminant D, we solve $\alpha^2 - 3\alpha\beta + \beta^2 = 0$ for α giving two solutions describing two lines with positive slopes,

$$\alpha = \frac{3 - \sqrt{5}}{2}\beta \text{ and } \alpha = \frac{3 + \sqrt{5}}{2}\beta.$$

The $\beta = \alpha$ line divides the positive quadrant of the (α, β) plane into two parts as shown in Figure 1. Each part is further divided into two parts by one of these two lines since the first line is steeper than the diagonal and the second

is flatter. Since the situation is symmetric with respect to the diagonal line, we focus on the left part to it by making the following assumption.

Assumption 3: $\alpha < \beta$

It is clear that in Figure 1, $D > 0$ in the left to the $\alpha = \frac{3-\sqrt{5}}{2}\beta$ line and $D < 0$ in the right.

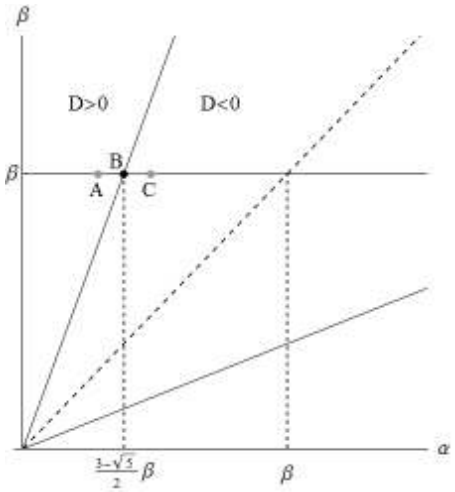

Figure 1. Division of the (α, β) plane

We reveal the effects caused by the changing values of the adjustment speeds on the shapes of the stability switching curves. Figures $2(A)$, (B) and (C) illustrate the $F(\omega)$ curves with $\beta = 1$,

$$\text{(A) } \alpha = \frac{3-\sqrt{5}}{2}\beta - 0.01, \text{ (B) } \alpha = \frac{3-\sqrt{5}}{2}\beta \text{ and (C) } \alpha = \frac{3-\sqrt{5}}{2}\beta + 0.01.$$

As is already mentioned in Theorem 2, $F(\omega)$ has a finite number of roots, in particular, there are four intersections with the axis of abscissa in Figure $2(A)$ with $D > 0$, two intersections and one tangency point in Figure $2(B)$ with $D = 0$ and two intersections in Figure $2(C)$ with $D < 0$.

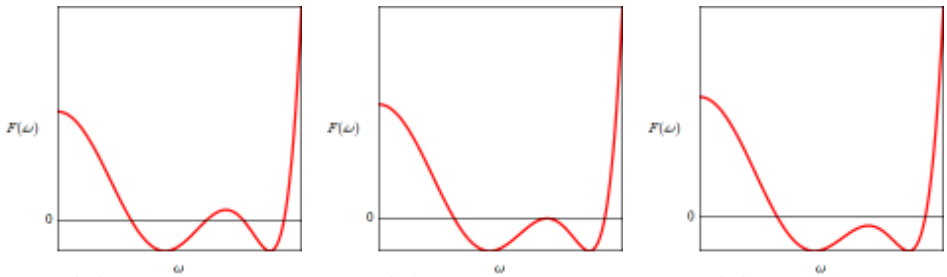

(A) Four roots (B) Three roots (C) Two roots

Figure 2. Shapes of $F(\omega)$

Accordingly, the corresponding stability switching curves are determined. For simplicity we confine attention to the case of $m = 0, 1$ and $n = 0$ and illustrate $L_R(0,0)$ and $L_B(1,0)$ as red and blue curves, respectively, in Figures 3(A), (B) and (C). We start with Figure 3(B), which is a boundary case between Figures 3(A) and 3(C). Since $D = 0$, $F(\omega) \leq 0$ for $\omega \in [\omega_2, \omega_1]$ with $\omega_2 < \omega_4 = \omega_3 < \omega_1$. The continuous red curve $L_R(0,0)$ consists of the two segments, one defined over the interval $[\omega_2, \omega_4]$ is unimodal and the other defined over the interval $[\omega_3, \omega_1]$ is positive-sloping. It has a kink at point (τ_x^0, τ_y^0) with

$$\tau_x^0 = \tau_x^+(\omega_m, 0) \text{ and } \tau_y^0 = \tau_y^-(\omega_m, 0)$$

where $\omega_m = \omega_4 = \omega_3$. In the same way, the blue curve $L_B(1,0)$ has two segments, one over $[\omega_2, \omega_4]$ has a steep positive slope and the other over $[\omega_3, \omega_1]$ has a flat negative slope. These segments are connected at the same kinked point,

$$\tau_x^0 = \tau_x^-(\omega_m, 1) \text{ and } \tau_y^0 = \tau_y^+(\omega_m, 1).$$

When the value of α increases from $(3 - \sqrt{5})\beta/2$, the discriminant becomes negative so the kinked point disappears. In consequence, $L_R(0,0)$ as well as $L_B(1,0)$ defined over interval $[\omega_2, \omega_3]$ become smoother as depicted in Figure 3(C). When the value of α decreases from $(3-\sqrt{5})\beta/2$, the discriminant becomes positive and the interval is separated into two distinct intervals, $[\omega_2, \omega_4]$ and $[\omega_3, \omega_1]$ with $\omega_3 > \omega_4$. Further, the kinked point (τ_x^0, τ_y^0) is broken into two different points, (τ_x^1, τ_y^1) and (τ_x^2, τ_y^2). In particular, the stability switching curve defined over $[\omega_2, \omega_4]$ takes an inequality-wise shaped curve and has the blue curve $L_B(1,0)$ connected with the red curve $L_R(0,0)$ at the point (τ_x^1, τ_y^1) where

$$\tau_x^1 = \tau_x^+(\omega_4, 0) = \tau_x^-(\omega_4, 1) \text{ and } \tau_y^1 = \tau_y^-(\omega_4, 0) = \tau_y^+(\omega_4, 1).$$

On the other hand, the stability switching curve defined over $[\omega_3, \omega_1]$ takes a flat-roof shaped curve and has the blue curve $L_B(1,0)$ connected with the red curve $L_R(0,0)$ at the point (τ_x^2, τ_y^2) where

$$\tau_x^2 = \tau_x^+(\omega_3, 0) = \tau_x^-(\omega_3, 1) \text{ and } \tau_y^2 = \tau_y^-(\omega_3, 0) = \tau_y^+(\omega_3, 1).$$

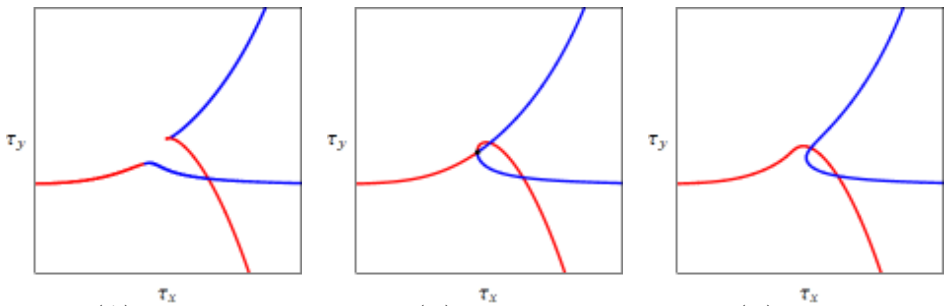

(A) $D > 0$ (B) $D = 0$ (C) $D < 0$

Figure 3. Stability crossing curves for $m = 0, 1$ and $n = 0$

3 Simulations

We now perform simulations to illustrate the theoretical findings. For this purpose, we specify some of the parameters in (1) as follows:

Assumption 4: $a = 4,\ b = 1,\ c_x = 1,\ c_y = 1$ and $\beta_y = 1$

Under this assumption, we have

$$x^e = y^e = 1,\ \beta = 1 \text{ and } \alpha = \alpha_x.$$

In Section 3.1, we take $\alpha_x = 0.5$ for which $D < 0$ as $(3 - \sqrt{5})/2 \simeq 0.382$, select three values of τ_y and examine how changing the value of τ_x affects dynamics generated by system (1). Then in Section 3.2, we decrease the value of α_x to 0.35 for which $D > 0$ and repeat the same procedure.

3.1 Simulation Study I

The adjustment coefficient of firm x is taken to be $\alpha_x = 0.5$ in this subsection. As in Figure 3(C), we have the smoother red curve $L_R(0,0)$ and the blue curve $L_B(1,0)$.[4] A larger value of α shifts the blue curve in Figure 3(C) rightward and the red curve leftward, resulting in the location of the curves as shown in Figure 4. Since it is shown that the stationary point is locally stable in the yellow region below the red curve, the red curve is the stability switching curve on which stability is lost. We select three different values of τ_y and perform three simulations with the increasing value of τ_x from zero to detect the effects caused by the delays.

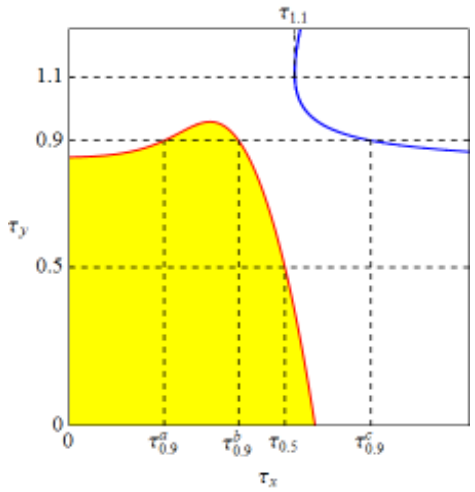

Figure 4. Division of the time delay plane

In the first example we take $\tau_y = 0.5$ and increase the value of τ_x along the dotted line that crosses the red curve at $\tau_x = \tau_{0.5} (\simeq 1.348)$ as shown in

[4] The segments of $L_B(0,0)$ and $L_R(1,0)$ do not appear in this region of (τ_x, τ_y).

Figure 4. A bifurcation diagram with respect to τ_x is given in Figure 5(A). It is constructed in the following way. With fixed value of τ_x, we run the delay system (1) with the specified parameter values for $0 \leq t \leq 1000$. To take away the initial disturbances, we discard the numerical data of $x(t)$ and $y(t)$ for $t \leq 950$ and plot the local maximum and local minimum of $y(t)$ obtained from the data for $950 \leq t \leq 1000$ against this value of τ_x. Then we increase the value of τ_x and repeat the same procedure until τ_x arrives at 2.8. It is shown there that until τ_x reaches $\tau_{0.5}$, the stationary point is asymptotically stable, loses stability at $\tau_x = \tau_{0.5}$ and a limit cycle of $y(t)$ emerges for $\tau_x > \tau_{0.5}$. To observe how cyclic fluctuations emerge, we gradually increase further the value of τ_x. We find first a unique minimum and maximum, then two minima and maxima, even further increase of τ_x results in three minima and maxima, and so on. Accordingly, we have a regular cycle, which is distorted more and more to be a cycle having several ups and downs by the increase of τ_x. For example, the vertical dotted line at $\tau_x = 2$ crosses the bifurcation diagrams eight times, four time with the upper branches of the diagram and four times with the lower branches. This implies that the motion of $y(t)$ is oscillatory and the trajectory has four increasing segments and four decreasing segments. In Figure 5(B) a periodic solution for $900 \leq t \leq 1000$ is illustrated in the (x, y) plane in red while the two best reply lines are shown in black.

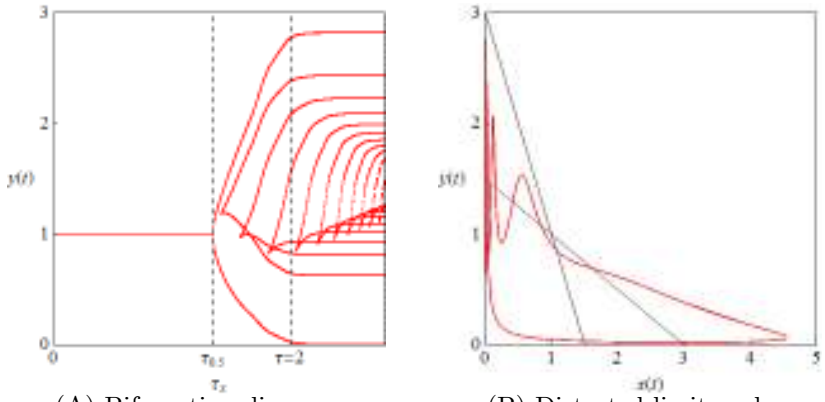

(A) Bifurcation diagram (B) Distorted limit cycle

Figure 5. Delay effects of τ_x, given $\tau_y = 0.5$

In the second example, we increase the value of τ_y to 0.9. The horizontal dotted line at $\tau_y = 0.9$ in Figure 4 crosses the red curve two times at $\tau_x = \tau^a_{0.9} (\simeq 0.593)$ and $\tau_x = \tau^b_{0.9} (\simeq 1.058)$ and the blue curve one time at $\tau_x = \tau^c_{0.9} (\simeq 1.885)$. A bifurcation diagram of $y(t)$ with respect to τ_x is given in Figure 6(A) and shows that increasing the value of τ_x along the dotted line gives rise to a wide variety of dynamics of $y(t)$ ranging from a stable trajectory to chaotic motions. There, a limit cycle emerges for $\tau_x < \tau^a_{0.9}$, stability is gained in the interval $(\tau^a_{0.9}, \tau^b_{0.9})$ for which the dotted line is located in the yellow region of Figure 4. Stability is lost again at $\tau_x = \tau^b_{0.9}$ and bifurcates to a periodic cycle having

several local maxima and minima for $\tau_x < \tau^c_{0.9}$ and finally more complicated dynamics arises for larger values of τ_x. Figure 6(B) illustrates a phase diagram for $9500 \leq t \leq 10000$ in the ($\log[x(t)]$,$\log[y(t)]$) plane for $\tau_x = \bar{\tau}(= 2)$ in which output exhibits many ups and downs.

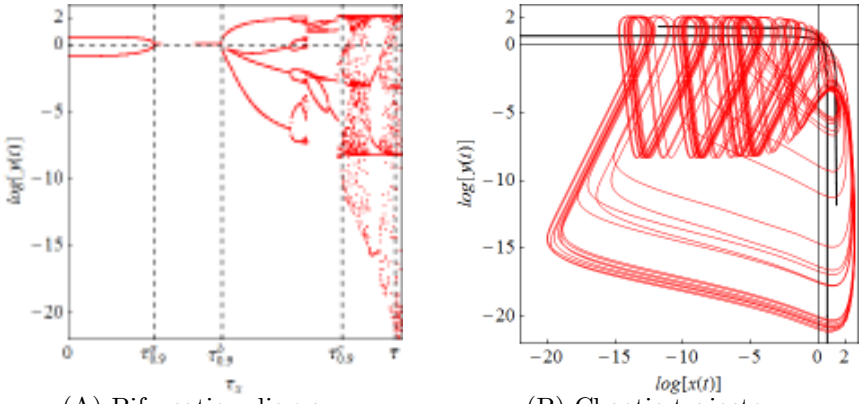

(A) Bifurcation diagram (B) Chaotic trajectory

Figure 6. Delay effects of τ_x, given $\tau_y = 0.9$

In the third example, the value of τ_y is further increased to 1.1 at which the dotted horizontal line starts and crosses the blue curve at $\tau_x = \tau_{1.1} (\simeq 1.409)$ in Figure 4. A bifurcation diagram shown in Figure 7(A) indicates that the steady state is locally unstable for $\tau_x = 0$ and the dynamic system (1) generates a limit cycle for $\tau_x > 0$. The limit cycle then bifurcates to complicated cycles through a period-doubling-like cascade and then comes back to a simple limit cycle through period-halving-like cascade for $\tau_x \leq \tau_{1.1}$. Further increasing τ_x indicates transformation to aperiodic oscillations from periodic oscillations. Figure 7(B) illustrates a phase diagrams of $\log[x(t)]$ and $\log[y(t)]$ for $9500 \leq t \leq 10000$ when $\tau_x = \bar{\tau}(= 2.25)$.

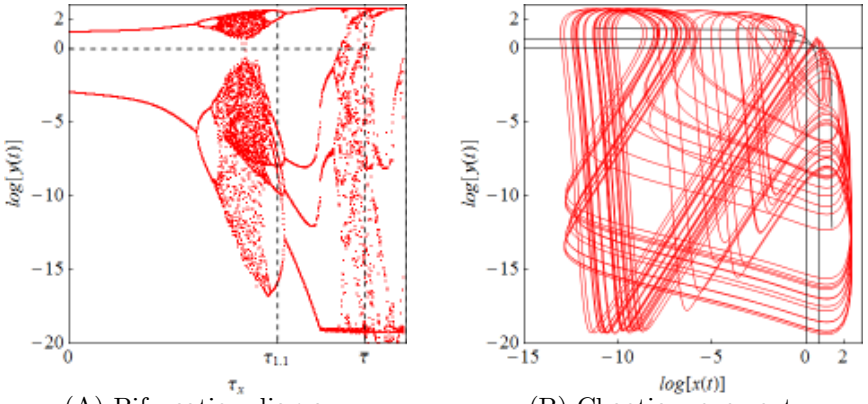

(A) Bifurcation diagram (B) Chaotic movement

Figure 7. Delay effects of τ_x, given $\tau_y = 1.1$

3.2 Simulation Study II

In this section we present numerical simulations when $\alpha = 0.35 < (3 - \sqrt{5})/2$. The last inequality implies $D > 0$ and as in Figure 3(A), there are two independent intervals, $[\omega_2, \omega_4]$ with $\omega_2 \simeq 0.563$ and $\omega_4 \simeq 1.081$ and $[\omega_3, \omega_1]$ with $\omega_3 \simeq 1.619$ and $\omega_1 \simeq 1.863$. For $\omega \in [\omega_2, \omega_4]$, the red curve $L_R(0,0)$ is connected to the blue curve $L_B(1,0)$ and thus both curves take distorted inequality-shaped profiles while only a small portion of the blue curve $L_B(1,0)$ is illustrated in Figure 8. On the other hand, for $\omega \in [\omega_3, \omega_1]$, the red curve $L_R(0,0)$ and the blue curve $L_B(0,0)$ together construct a flatterly roof-shaped profile. In the yellow region surrounded by these curves, the stationary point is locally stable and its stability is lost on these curves. To examine what kinds of dynamics emerge for (τ_x, τ_y) in the white region, we will perform three numerical simulations as before.

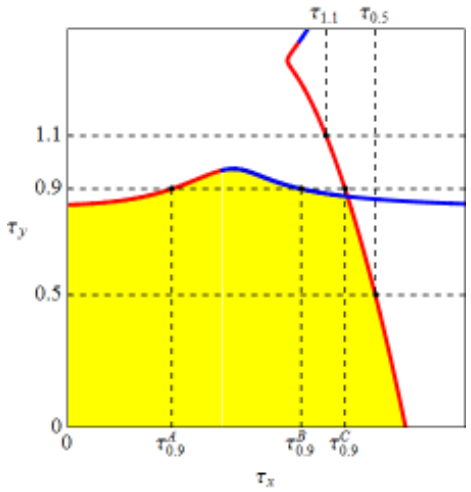

Figure 8. Dividion of the (τ_x, τ_y) plane

In the first simulation, we take $\tau_y = 0.5$ and increase the value of τ_x along the dotted line that crosses the downward sloping red curve at $\tau_x = \tau_{0.5} (\simeq 1.934)$ in Figure 8. A bifurcation diagram is presented in Figure 9(A) in which the dynamics seems to be similar to the one in Figure 5(A), that is, stability is lost at $\tau_x = \tau_{0.5}$ and a limit cycle is born for $\tau_x > \tau_{0.5}$. It is seen that the number of increasing and decreasing segments increases as the value of τ_x increases. In Figure 9(B) a time trajectory of $y(t)$ for $955 \leq t \leq 1000$ is depicted when $\tau_x = 3$. Within one cycle, the trajectory hits maximum and minimum seven times each.

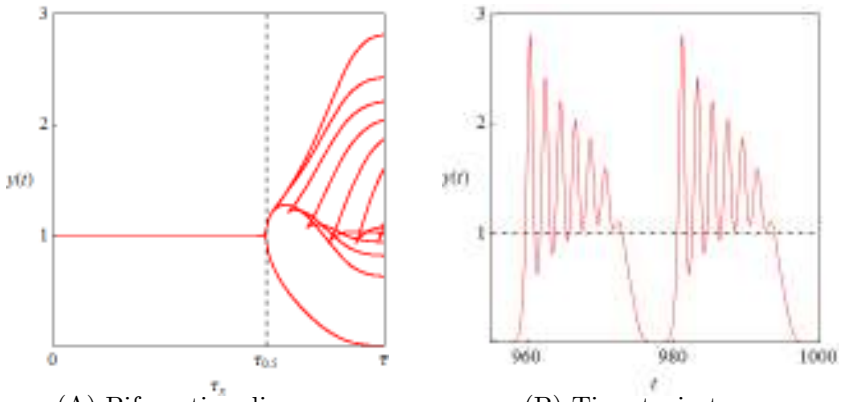

(A) Bifurcation diagram (B) Time trajectory

Figure 9. Delay effect of τ_x, given $\tau_y = 0.5$

In the second example, τ_y is increased to 0.9. As can be seen in Figure 8, the dotted line at $\tau_y = 0.9$ crosses the positive-sloping red curve at $\tau_x = \tau_{0.9}^A (\simeq 0.954)$, the negative sloping blue curve at $\tau_x = \tau_{0.9}^B (\simeq 1.467)$ and the

negative sloping red curve at $\tau_x = \tau^C_{0.9} (\simeq 1.743)$. So as the value of τ_x increases from zero, the stationary state gains stability for $\tau^A_{0.9} < \tau_x < \tau^B_{0.9}$ and loses it otherwise. The bifurcation diagram presented in Figure 10(A) reveals what kind of dynamics emerges when stability is lost. A simple limit cycle arises for $\tau_x < \tau^A_{0.9}$ while more complex dynamics emerges via a period-increasing cascade for $\tau_x > \tau^B_{0.9}$. With further increasing the value of τ_x, a very long periodic cycle or chaotic behavior might emerge and its oscillations are aperiodic but not erratic. Figure 10(B) gives time trajectories for $\tau_x = \bar{\tau} (= 2.8)$, the red one for $\log[y(t)]$ and the blue one for $\log[x(t)]$. A phase diagram in the $(\log[x(t)], \log[y(t)])$ plane is very similar to the one shown in Figure 9(B).

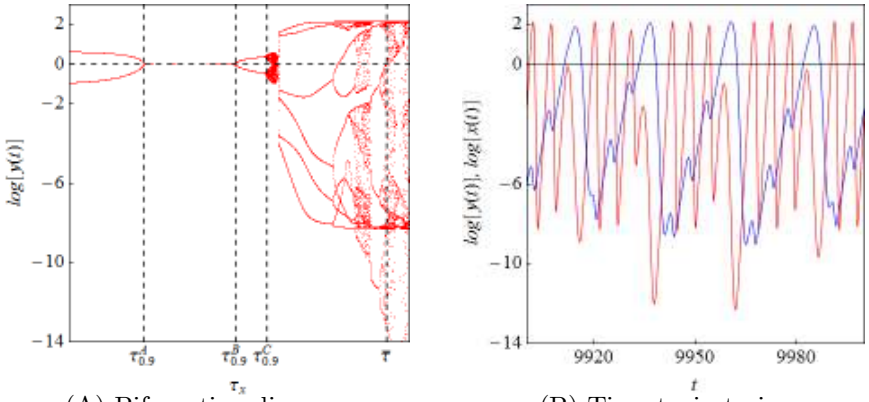

(A) Bifurcation diagram (B) Time trajectories

Figure 10. Delay effect of τ_x, given $\tau_y = 0.9$

In the third example, τ_y is further increased to 1.1 at which the dotted horizontal line crosses the positive-sloping segment of the red curve at $\tau_x = \tau_{1.1} (\simeq 1.624)$. Since the line is located in the white region of Figure 8, the stationary state is locally unstable for any $\tau_x \geq 0$ and a bifurcation diagram in Figure 11(A) shows that periodic and aperiodic motions of $y(t)$ alternate as the value of τ_x increases. The time trajectories of $\log[x(t)]$ and $\log[y(t)]$ at $\tau_x = \bar{\tau} (= 2.5)$ are illustrated again as the blue and the red curves in Figure

11(B). They are aperiodic but not erratic.

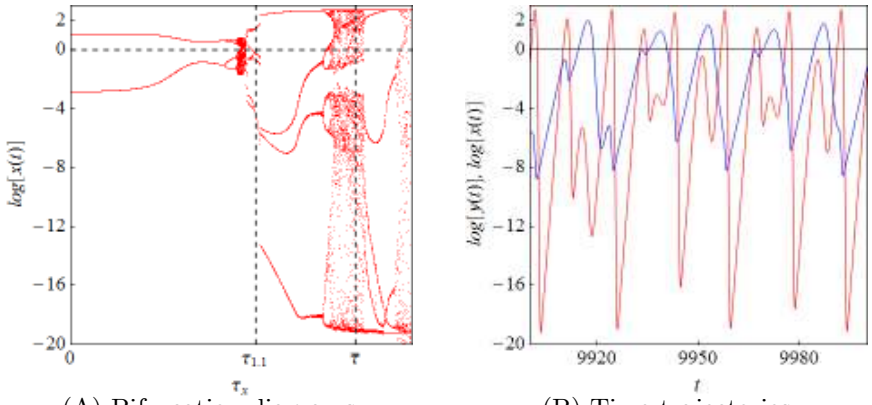

(A) Bifurcation diagrams (B) Time trajectories

Figure 11. Delay effect of τ_x, given $\tau_y = 1.1$

4 Concluding Remarks

In this paper we have focused on dynamics of the Cournot duopoly model in which each firm has a delay in implementing information about its own output. First we analytically derived the stability switching curve that divides the delay region into two regions, one in which stability is preserved and the other in which stability is lost. Then we numerically examined dynamic behavior of output when the stationary state loses stability. It is found that the shape of the stability switching curve is parameter-dependent. It is demonstrated that the two delay model can generate rich dynamics involving chaotic oscillations. This finding implies that the delay can be a source of periodic as well as aperiodic dynamics in the continuous-time framework. It may be possible to extend the numerical results in the cases of higher dimension. However the construction of the stability switching surfaces in higher dimesions is still in progress.

Appendix

Following Lin and Wang (2012), we now present the proof of Theorem 1. Since $\left|e^{-i\omega\tau_x}\right| = \left|e^{-i\omega\tau_y}\right| = 1$, equations (4) and (5) can be written as

$$\left|P_0(i\omega) + P_1(i\omega)e^{-i\omega\tau_x}\right| = \left|P_2(i\omega) + P_3(i\omega)e^{-i\omega\tau_x}\right|$$

and

$$\left|P_0(i\omega) + P_2(i\omega)e^{-i\omega\tau_y}\right| = \left|P_1(i\omega) + P_3(i\omega)e^{-i\omega\tau_y}\right|.$$

Using the relation

$$\left|a + be^{-i\omega\tau}\right|^2 = \left(a + be^{-i\omega\tau}\right)\left(\bar{a} + \bar{b}e^{i\omega\tau}\right),$$

we can rewrite (4) as

$$|P_0|^2 + |P_1|^2 - |P_2|^2 - |P_3|^2 = 2A_1(\omega)\cos(\omega\tau_x) - 2B_1(\omega)\sin(\omega\tau_x) \qquad \text{(A-1)}$$

and (5) as

$$|P_0|^2 - |P_1|^2 + |P_2|^2 - |P_3|^2 = 2A_2(\omega)\cos(\omega\tau_y) - 2B_2(\omega)\sin(\omega\tau_y) \qquad \text{(A-2)}$$

where

$$A_1(\omega) = \mathrm{Re}[P_2\bar{P}_3 - P_0\bar{P}_1] \text{ and } B_1(\omega) = \mathrm{Im}[P_2\bar{P}_3 - P_0\bar{P}_1]$$

and

$$A_2(\omega) = \mathrm{Re}[P_1\bar{P}_3 - P_0\bar{P}_2] \text{ and } B_2(\omega) = \mathrm{Im}[P_1\bar{P}_3 - P_0\bar{P}_2].$$

It is clear that both $P_2\bar{P}_3 - P_0\bar{P}_1$ and $P_1\bar{P}_3 - P_0\bar{P}_2$ are pure complex with zero real parts. So $A_1(\omega) = A_2(\omega) = 0$. Assume $B_1(\omega) \neq 0$ and $B_2(\omega) \neq 0$ and then compute the arguments of these complex values as

$$\varphi_x(\omega) := \arg(P_2\bar{P}_3 - P_0\bar{P}_1) = \begin{cases} \dfrac{\pi}{2} \text{ if } B_1(\omega) > 0, \\ \dfrac{3\pi}{2} \text{ if } B_1(\omega) < 0 \end{cases}$$

and

$$\varphi_y(\omega) := \arg(P_1\bar{P}_3 - P_0\bar{P}_2) = \begin{cases} \dfrac{\pi}{2} \text{ if } B_2(\omega) > 0, \\ \dfrac{3\pi}{2} \text{ if } B_2(\omega) < 0. \end{cases}$$

With $A_1(\omega) = 0$ and $\cos\varphi_x(\omega) = 0$, the right-hand side of equation (A-1) can be rewritten as

$$\begin{aligned} -2B_1(\omega)\sin\omega\tau_x &= -2\left|B_1(\omega)\right|\sin\varphi_x(\omega)\sin\omega\tau_x \\ &= 2\left|B_1(\omega)\right|\left[\cos\varphi_x(\omega)\cos\omega\tau_x - \sin\varphi_x(\omega)\sin\omega\tau_x\right] \\ &= 2\left|B_1(\omega)\right|\cos[\varphi_x(\omega) + \omega\tau_x]. \end{aligned}$$

The right-hand side of equation (A-2) can be rewritten in the same way. Therefore, (A-1) and (A-2) becomes

$$|P_0|^2 + |P_1|^2 - |P_2|^2 - |P_3|^2 = 2\,|B_1(\omega)|\cos(\varphi_x(\omega) + \omega\tau_x) \tag{A-3}$$

and

$$|P_0|^2 - |P_1|^2 + |P_2|^2 - |P_3|^2 = 2\,|B_1(\omega)|\cos(\varphi_y(\omega) + \omega\tau_y). \tag{A-4}$$

A sufficient and necessary condition for the existence of $\tau_x > 0$ and $\tau_y > 0$ satisfying the above equations are

$$\left||P_0|^2 + |P_1|^2 - |P_2|^2 - |P_3|^2\right| \leq 2\,|B_1(\omega)| \tag{A-5}$$

and

$$\left||P_0|^2 - |P_1|^2 + |P_2|^2 - |P_3|^2\right| \leq 2\,|B_1(\omega)|\,. \tag{A-6}$$

Denote by Ω^1 and Ω^2 the set of $\omega > 0$ values satisfying (A-5) and (A-6), respectively. Let us define new functions by

$$\cos[\psi_x(\omega)] = \frac{|P_0|^2 + |P_1|^2 - |P_2|^2 - |P_3|^2}{2\,|B_1(\omega)|},\ \psi_x \in [0, \pi] \tag{A-7}$$

and

$$\cos[\psi_y(\omega)] = \frac{|P_0|^2 - |P_1|^2 + |P_2|^2 - |P_3|^2}{2\,|B_1(\omega)|},\ \psi_y \in [0, \pi], \tag{A-8}$$

then from (A-3) and (A-7), (A-4) and (A-8), we have

$$\cos[\varphi_x(\omega) + \omega\tau_x] = \cos[\psi_x(\omega)]$$

and

$$\cos[\varphi_y(\omega) + \omega\tau_y] = \cos[\psi_y(\omega)]$$

both of which yield, for arbitrary integers m and n,

$$\tau_x^{\pm}(\omega, m) = \frac{\pm\psi_x(\omega) - \varphi_x(\omega) + 2m\pi}{\omega}$$

and

$$\tau_y^{\pm}(\omega, n) = \frac{\pm\psi_y(\omega) - \varphi_y(\omega) + 2n\pi}{\omega}.$$

These are the values of the delays that solve equations (4) and (5). Therefore, given m and n, $(\tau_x^+(\omega, m), \tau_y^-(\omega, n))$ for $\omega \in \Omega^1$ and $(\tau_x^-(\omega, m), \tau_y^+(\omega, n))$ for $\omega \in \Omega^2$ construct the stability switching curves in the (τ_x, τ_y) plane. Q.E.D.

References

Bischi, G-I, Chiarella, C., Kopel, M. and Szidarovszky, F. *Nonlinear Oligopolies: Stability and Bifurcations*, 2010, Heidelberg Dordrecht, London, New York, Springer.

Cournot, A. *Recherches sur les Principes Mathématiques de la Théorie des Richessess*, 1838, Hachette, Paris (English translation (1960): *Researches into the Mathematical Principles of the Theory of Wealth*, Kelley, New York).

Hofbauer, J. and So, J. Diagonal Dominance and Harmless Off-diagonal Delays, *Proceedings of the American Mathematical Society*, 128, 2000, 2675-2682.

Howroyd, T. and Russell, A. Cournot Oligopoly Models with Time Delays, *Journal of Mathematical Economics,* 13, 1984, 7-103.

Lin, X. and Wang, H., Stability Analysis of Delay Differential Equations with Two Discrete Delays, *Canadian Applied Mathematics Quarterly*, 20, 2012, 519-533.

Matsumoto, A. and Szidarovszky, F. Learning Monopolies with Delayed Feedback on Price Expectations, *IERCU Discussion Paper* #223 (http://www.chuo-u.ac.jp/research/institutes/economic/publication/discussion/pdf/discussno223.pdf), Institute of Economic Research, Chuo University, 2014a.

Matsumoto, A. and Szidarovszky, F., Discrete and Continuous Dynamics in Nonlinear Monopolies, *Applied Mathematics and Computation*, 232, 632-642, 2014b.

Matsumoto, A., Szidarovszky, F. and Yoshida, H. Dynamics in Linear Cournot Duopolies with Two Time Delays, *Computational Economics*, 38, 2011, 311-327.

Okuguchi, K. *Expectations and Stability in Oligopoly Models*, 1976, Berlin, Springer.

Okuguchi, K. and Szidarovszky, F. *The Theory of Oligopoly with Multi-product Firms* (2nd ed), 1999, Berlin, Springer.

Shibata, A. and Saito, N. Time Delays and Chaos in Two Competitng Species, *Mathematical Biosciences*, 51, 1980, 199-211